IEEE Photonics Journal
An IEEE Photonics Society Publication

Open Access

Bright and Dark Square Pulses Generated From a Graphene-Oxide Mode-Locked Ytterbium-Doped Fiber Laser

Volume 6, Number 3, June 2014

Rong-yong Lin
Yong-gang Wang
Pei-guang Yan
Ge-lin Zhang
Jun-qing Zhao
Hui-quan Li
Shi-sheng Huang
Guang-zhong Cao
Ji-an Duan

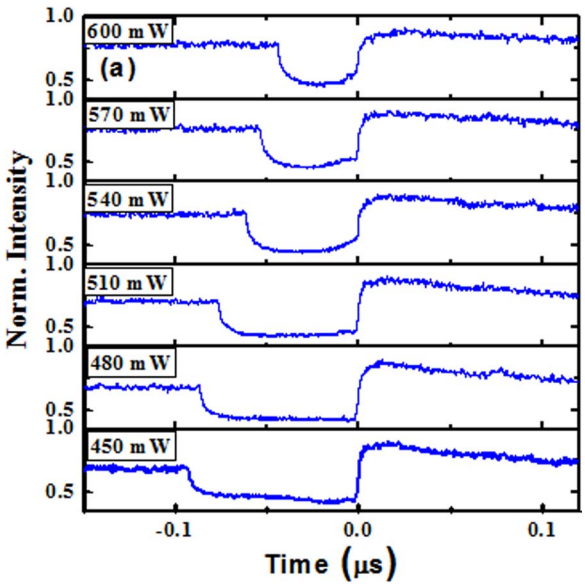

DOI: 10.1109/JPHOT.2014.2319099
1943-0655

IEEE photonics SOCIETY

IEEE

Bright and Dark Square Pulses Generated From a Graphene-Oxide Mode-Locked Ytterbium-Doped Fiber Laser

Rong-yong Lin,[1] Yong-gang Wang,[2] Pei-guang Yan,[1] Ge-lin Zhang,[1] Jun-qing Zhao,[1] Hui-quan Li,[1] Shi-sheng Huang,[1] Guang-zhong Cao,[3] and Ji-an Duan[4]

[1]Shenzhen Key Laboratory of Laser Engineering, Key Laboratory of Advanced Optical Precision Manufacturing Technology of Guangdong Higher Education Institutes, College of Electronic Science and Technology, Shenzhen University, Shenzhen 518060, China
[2]The State Key Laboratory of Transient Optics and Photonics, Xi'an Institute of Optics and Precision Mechanics, Chinese Academy of Sciences, Xi'an 710119, China
[3]Shenzhen Key Laboratory of Electromagnetic Control, Shenzhen University, Shenzhen 518060, China
[4]State Key Laboratory of High Performance Complex Manufacturing, Central South University, Changsha 410083, China

DOI: 10.1109/JPHOT.2014.2319099

Manuscript received April 1, 2014; accepted April 11, 2014. Date of publication April 29, 2014; date of current version May 6, 2014. This work was supported by the Natural Science Fund of Guangdong Province under Grant S2013010012235; by the Foundation for Scientific and Technical Innovation in Higher Education of Guangdong under Grant 2013KJCX0161; by the Improvement and Development Project of Shenzhen Key Laboratory under Grant ZDSY20120612094924467; by the Science and Technology Project of Shenzhen City under Grants JCYJ20120613172042264 and JCYJ20130329142040731; by the Natural Science Foundation of SZU under Grant 201221; and by the Open Research Fund of the Key Laboratory of High Performance Complex Manufacturing, Central South University, under Grant HPCM-2013-10. Corresponding author: P. Yan (e-mail: yanpg@szu.edu.cn).

Abstract: The observation of the bright pulses and dark square pulses in a graphene-oxide saturable absorber (GOSA) passively mode-locked ytterbium-doped fiber laser has been investigated experimentally. Bright pulses are achieved at a pump power of ~200 mW. However, the dark-square-pulse generation starts at a much higher pump power of ~450 mW. At the maximum pump power of 600 mW, the dark-square-pulse bunches and harmonic mode locking (HML) can be also obtained by tuning the polarization controller (PC) to different orientations. It is the first demonstration of the bunches and HML of dark square pulses in a GOSA passively mode-locked ytterbium-doped fiber laser with large normal dispersion cavity.

Index Terms: Graphene-oxide, mode-locked fiber laser, dark square pulse, dark square pulse bunches, harmonic mode-locking.

1. Introduction

It was well known that Q-switching or mode-locking in a passively fiber laser generated bright pulses originally [1], [2], and it would be interesting to know that a passively fiber laser could emit dark pulses. Bright and dark solitons could be governed by the nonlinear Schrödinger equation (NLSE) [3]. Dark solitons are also solutions of the complex Ginzburg-Landau equation (CGLE) [4], [5]. In particular, in the anomalous dispersion SMFs, bright solitons could be formed, while in the normal dispersion SMFs, dark solitons, characterized as a localized intensity dip on a continuous

wave (CW) background [6], could be formed. Compared with bright soliton, numerical simulations revealed that dark solitons spread more slowly in the presence of fiber loss and could be more stable in the presence of noise. Furthermore, some experimental results pointed out that dark soliton could be generated and maintained over considerable fiber length [7]. The above listed features indicated that dark solitons would have some better applications in optical-processing systems [8]. For example, the dark-pulse laser was envisioned as a tool for infra-red (IR) communications and measurements [9]. Dark pulses could be useful in signal processing and could be also used like a camera shutter for a CW light beam in optical networks [9]. Atom optical clock would be more widely applied if the dark pulse lasers could achieve a much smaller size and a simpler structure [10]. Recently, dark solitons have been observed in mode-locked fiber lasers. Quiroga-Teixeiro *et al.* [11] theoretically investigated a mode-locking mechanism by dissipative four-wave mixing and predicted the formation of a dark soliton in the laser. The direct generation of dark pulses in a mode-locked fiber cavity was firstly demonstrated by Sylvestre *et al.* [12]. Then, Zhang *et al.* [13] have experimentally demonstrated single and multiple dark pulse emission in an all-anomalous fiber ring laser with the nonlinear polarization rotation (NPR) technique for mode locking. Later, the observation of dark pulses were demonstrated in dispersion-managed (DM) fiber ring lasers with either net normal or net anomalous cavity group velocity dispersion (GVD) [14], [15]. In addition, several new types of dark pulses were theoretically predicted and experimentally observed in fiber lasers [16]–[19]. Tang *et al.* [20] not only experimentally confirmed the existence of dark solitons in the fiber laser but also identified that the dark pulses observed previously were bunches of the dark solitons and showed that the dark soliton formation is a generic feature of the all-normal-dispersion-fiber lasers. Gao [21] has demonstrated the generation of the fundamental dark square pulses in a ring cavity with a 207-m long tellurite single-mode fiber which could provide the high nonlinearity, high birefringence, and large normal dispersion for the formation of the dark square pulse. In addition, as an important technique to increase the dark pulse repetition rate, the relevant HML fiber lasers have been a particularly attractive and growing research region. The dark pulses with tunable repetition rate were experimentally observed from an EDF ring laser [22]. Dark pulses and their HML counterparts have also been obtained in an ytterbium-doped fiber (YDF) ring laser with a long cavity [23].

Recently, GO has been widely investigated as novel SAs due to its own chemical characteristics and physical. As far as what we knew, it has been successful in hundreds of demonstrations that using graphene-oxide saturable absorber (GOSA) for the realization of mode-locking [24]–[29], and most the existing results were about bright pulses. However, no references about dark square pulses emission from the mode-locking fiber lasers using GO as SA were reported.

In this letter, besides the bright pulses, we have also demonstrated the dark square pulse in a GOSA passively mode-locked YDF laser with large normal dispersion cavity. Dark square pulse bunches and HML are also obtained by rotating the orientations of the polarization controller (PC) at the maximum pump of 600 mW.

2. Sample Preparation and Experimental Setup

The fabrication method of GO-based SA is similar to our previous works [30]–[32]. The flake of the oxidized graphite is about $1 \sim 3$ atomic layers and $0.1 \sim 5.0$ μm of the diameter. At the first step, $\sim$0.6-mg GO powder was poured into $\sim$10 ml 0.1% sodium dodecyl sulfate (SDS) aqueous solution with ultrasonic agitation for more than 10 h and centrifugation for removing large GO clusters. Then, the upper portion of the prepared solution was decanted and then mixed with 0.4-g poly vinyl alcohol (PVA) powder with ultrasonic agitation for 3 h at $\sim$90 °C. Lastly, the GO/PVA solution was vertically evaporated in a polystyrene cell for about 2 days at $\sim$40 °C. The GO/PVA film was obtained after separation with the polystyrene cell, as shown in the inset of Fig. 1(a). It can be seen that both the GO concentration and film thickness increased from the top to the bottom due to the increasing evaporation time experienced. The thicknesses of the GO/PVA film can vary between 20 μm and 120 μm. The prepared GOSA was cut in $\sim 1 \times 1$ mm^2 small pieces, then we sandwiched one piece which with relatively higher thickness and concentration between two fiber

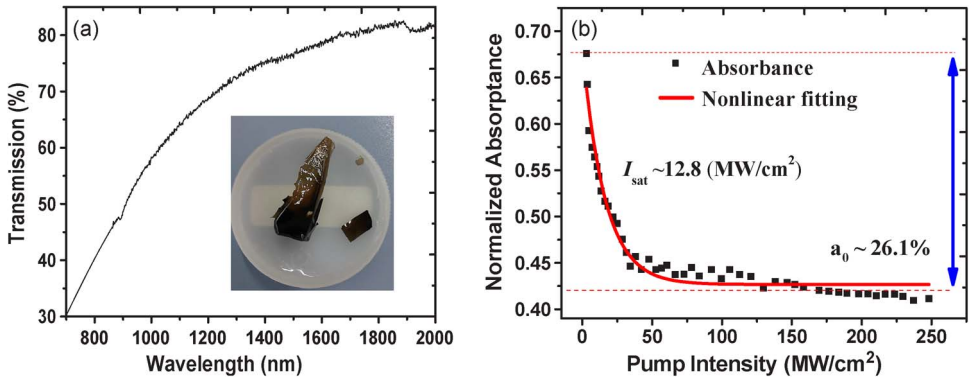

Fig. 1. (a) Linear transmission curves of the GO cell. (b) Nonlinear absorbance of the utilized GOSA piece.

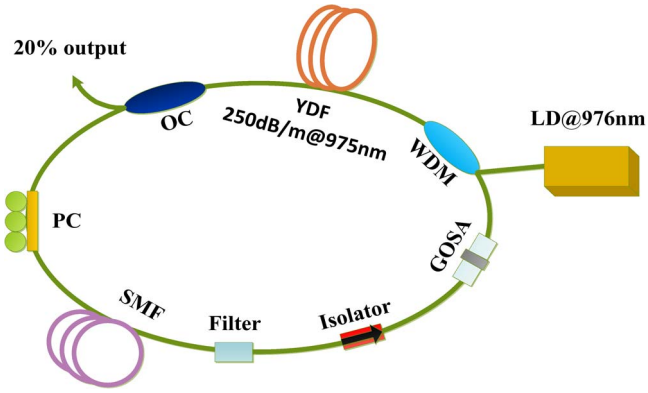

Fig. 2. A schematic diagram of the fiber ring laser. ISO: isolator, WDM: wavelength division multiplexer, OC: optical coupler, YDF: Yb-doped fiber, PC: polarization controller, SMF-28: single mode fiber, GOSA: graphene oxide saturable absorber.

connectors (FC-PC) in the cavity. An UV/Vis Spectrometer (Perkin Elmer, lambda 950) was employed to measure the linear optical transmission of the GO cell, as shown in Fig. 1(a). The saturable absorption property of the GO was shown in Fig. 1(b). The laser source used was a homebuilt mode-locked oscillator with 5 MHz repetition rate and 150 ps pulse duration operating at about 1064 nm. The date obtained from the experiment was then fitted according to

$$\alpha(I) = \alpha_0 \left(1 + \frac{I}{I_{\text{sat}}}\right)^{-1} + \alpha_{\text{ns}} \tag{1}$$

where I is the input laser intensity, I_{sat} is the saturation intensity (the intensity with the absorption coefficient of half the initial value), $\alpha(I)$ is the intensity-dependent absorption coefficient, and α_0 and α_{ns} are the modulation depth and the non-saturable loss, respectively. The results give a saturation intensity of ~12.8 MW/cm^2, modulation depth of ~26.1%, and non-saturable loss of ~42.2%.

The experimental configuration is shown in Fig. 2. The all-fiber ring laser cavity features 976-nm pumping of a 1.4-m-long YDF (core absorption of 250 dB/m@975 nm and GVD parameter of -27.5 ps^2/km@1060 nm) through a fused 980/1060 wavelength division multiplexer (WDM) coupler, with a maximum pump power of 600 mW. A polarization insensitive optical isolator (ISO) is inserted in laser cavity to ensure unidirectional operation, and a three-spool PC is employed to control the polarization state of the pulses. A 20/80 fused fiber optical coupler (OC) is used to extract ~20% energy from the cavity for signal detection. A bandwidth filter with a central wavelength of 1064 nm and 3 dB bandwidth of ~5 nm is inserted into the cavity for suppressing the

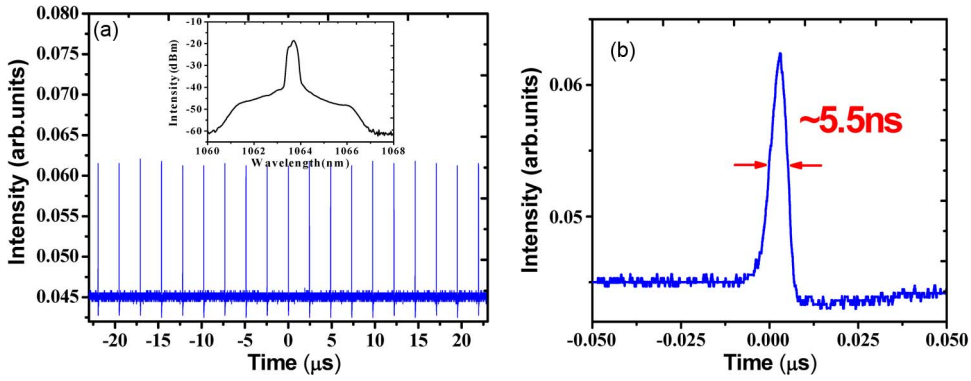

Fig. 3. (a) Oscilloscope trace. (b) Single pulse. Inset: Corresponding spectrum.

mode competition effect. The prepared GO-based SA is sandwiched between two fiber connectors. All these components are made of SMF-28 or pigtailed with SMF-28. ~490 m length of SMF-28 is incorporated to lengthen the cavity. The GVD parameter of SMF-28 is ~17.7 ps^2/km at 1064 nm. The total cavity length is ~492 m; thus, the net dispersion of the laser cavity is estimated ~8.645 ps^2. The monitoring of the output temporal pulse trains and optical spectrum is performed using a 1-GHz digital phosphor oscilloscope (Tektronix DPO7104C) and an optical spectrum analyzer (OSA, AQ6370B) with a minimum resolution of 0.02 nm. The pump power and output power are monitored by a photodiode power meter (COHERENT).

3. Experimental Results and Discussion

3.1. Bright Pulse

The laser threshold pumping power for CW operation was ~147 mW. The fundamental mode-locking operation was achieved by increasing the pump power to ~200 mW and with an appropriate setting of the PC. As shown in Fig. 3(a), the fundamentally pulse train had a uniform pulse interval of ~2.408 μs, corresponding to the cavity roundtrip time, which was determined by the cavity length. The repetition rate of the laser was ~415.3 kHz. The figure inset showed that the corresponding central wavelength was 1063.7 nm, and the 3-dB spectral bandwidth was 0.35 nm. The Fig. 3(b) showed the full width at half maximum (FWHM) of the bright pulse was ~5.5 ns.

3.2. Dark Square Pulse

At pump power of 450 mW, the laser emission could be tuned from the bright pulse emission first to a CW operation state, and then to a dark pulse emission state by continuously adjusting the PC. The corresponding oscilloscope trace was shown in Fig. 4(b), which represented as a narrow intensity dip in the strong CW laser emission background. The corresponding repetition rate was ~415.3 kHz. Although the formation of dark pulse was away from mode-locking [13], [18] and was due to modulation instability [33], the saturation effect was still needed, which could be approved by the numerical simulations by Zhang *et al.* [18]. It has been proved that graphene saturable absorber (GSA) could play its role in the generation of dark pulses by providing saturation effect in our previous works [34]. We were unable to obtain the dark square pulses without the GOSA in the cavity, so we believed that the GOSA could also play a role to emit dark square pulses by providing saturation effect in our cavity. In addition, as pointed in ref. [21] that the role of the 207 m long tellurite fiber in their cavity was decisive because it simultaneously provided the high nonlinearity, high birefringence, and large normal dispersion, all of which were crucial for the formation of a dark square pulse and were difficult to implement in a silica fiber of a short length on the order of several hundred meters. Although lacking of a tellurite fiber in our cavity, the total cavity length was ~492 m, which may also provide enough nonlinearity, birefringence, and normal dispersion, in combination

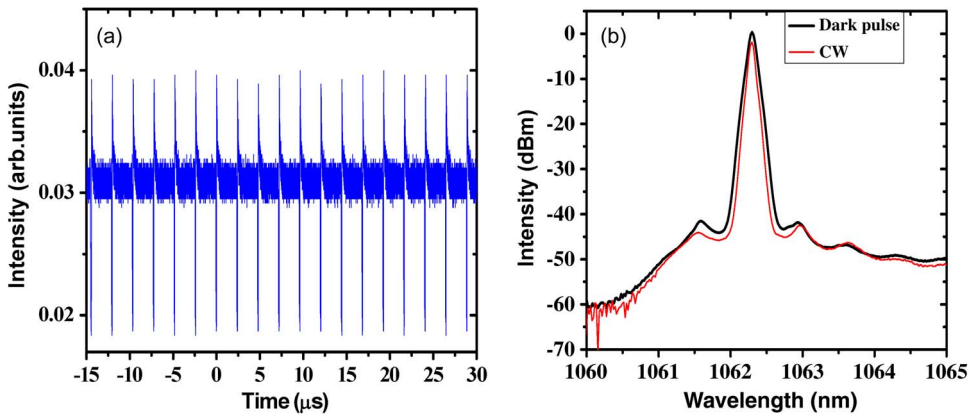

Fig. 4. Typical oscilloscope traces of bright pulse. (a) Typical oscilloscope traces of dark pulse. (b) Spectra of the dark pulse and of the CW operation state at a pump power of 450 mW.

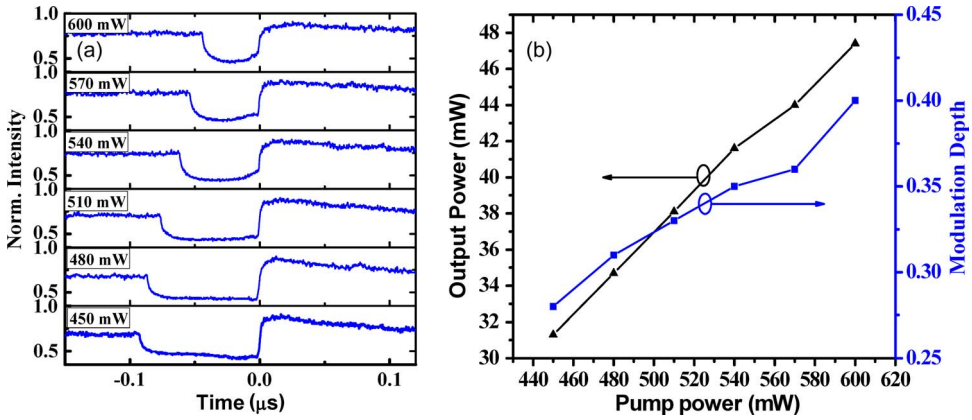

Fig. 5. (a) The dark square pulses durations under different pump powers. (b) Output powers and modulation depth versus the pump powers.

with the GOSA, caused the dark square pulse formation. In our experiment, the co-existence of much weaker bright pulses was exactly a sign of weak mode-locking by adjusting the PC properly (associated with the birefringence of the cavity) and changing the pump power (associated with the cavity gain). Fig. 4(b) showed the laser emission spectra in CW regime (a red curve) and in dark pulse regime (a black curve) at pump power of 450 mW. It was observed that the laser emission spectrum of the dark pulse was slightly broader, which was due to the nonlinear and dispersive effected.

The single pulse width of dark pulse could be detected by a 1 GHz digital phosphor oscilloscope because the pulse width of dark pulse was broader than the nanosecond scale [20]. Media 1 showed the recorded dark pulses trains at pump power of 450 mW. It could be seen that the dark pulse had a square shape, which was termed as dark square pulse here, and no fine structure was observed in the dark square pulse due to no intrinsic modulation instability existed. By fixing the PC, the duration of dark square pulse could be tuned by changing the pump power. We recorded the evolution of single pulse width as shown in Fig. 5(a). At pump powers of 450 mW, 480 mW, 510 mW, 540 mW, 570 mW, and 600 mW, the corresponding pulse durations were 90.80 ns, 84.70 ns, 74.55 ns, 59.70 ns, 51.55 ns, and 42.05 ns, respectively. Worth mention was that the accompanied bright pulse became much weaker in this process, indicating the operation condition was closer to the non-mode-locking regime at higher pump power. As a result, the square shape of the dark pulse could be optimized by approximately increasing the pump power. Fig. 5(b)

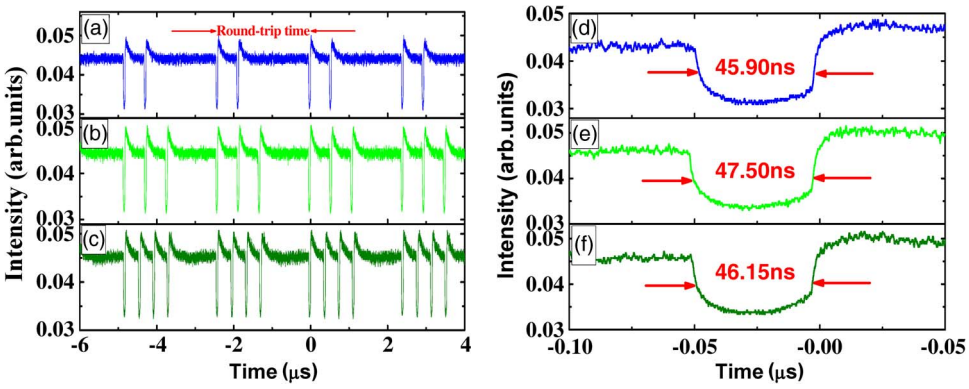

Fig. 6. The three kinds of dark square pulses bunches [(a)–(c)] and their corresponding single pulse [(d)–(f)].

exhibited the modulation depth which defined as the ratio of the minimal power of the dark pulse to the CW level and output power and with respect to the pump power. As can be seen, the output power almost linearly increased with the pump power, and reached to 47.40 mW at the maximum pump. The modulation depth became deeper from ∼28% to ∼40% as the pump power increased.

3.3. Bunches and HML of Dark Square Pulse

At the maximum 600 mW, new dark square pulses was found to be generated directly from the background noise by adjusting the PC carefully. Then the dark square pulse bunches would be observed. Finally, we obtained different types of bunches in which 2, 3 or 4 dark pulses coexisted in a round-trip time, as was shown in Fig. 6(a)–(c). Each bunch simultaneously had the same shallowness, indicating that their darkness was the same. At the same time, the space between one to another dark square pulse in each bunch was equally, and the dark square pulses in each bunch maintained the same modulation depth. Their corresponding single pulse durations were measured as 45.90 ns, 47.50 ns, 46.15 ns as shown in Fig. 6(d)–(f). The repetition rates of the three kinds of bunches were approximately equal to the fundamental repetition rate of ∼415.3 kHz.

Adjusting the PC carefully at the maximum pump power of 600 mW again, the bunch of dark square pulses would be unstable. Splitting of dark square pulses would occur or some new dark square pulses were generated directly from the background noise again. Then the new dark square pulses were unstable and rearranged themselves automatically. Eventually, new harmonic component was observed in the oscilloscope. Operation modes with the HML counterparts of dark square pulse of orders 2, 6, and 8 were shown in Fig. 7(a)–(c), and the corresponding repetition rate were ∼0.8436 MHz, ∼2.4840 MHz, and ∼3.3740 MHz, respectively.

P. Grelu had pointed out that high accumulated nonlinearity could lead to pulses splitting [35]. A ∼490 m length of SMF was incorporated into our cavity could provide enough nonlinearity to lead to the pulse splitting occur more easily. Dark square pulses in the cavity firstly went through the effect of dispersion and nonlinearity at a strong pumping of 600 mW. Then splitting of the dark square pulses would occur when the PC at an appropriate orientation, and new dark square pulses were unstable. And then, the relative phase and the interaction between the new pulses played a key role in the process. Finally, dark square pulse bunches and harmonic mode-locking would be obtained.

4. Conclusion

We have reported on the experimental observations of the bright pulses and dark square pulse in a GOSA passively mode-locked YDF laser with large normal dispersion cavity. The dark square pulse

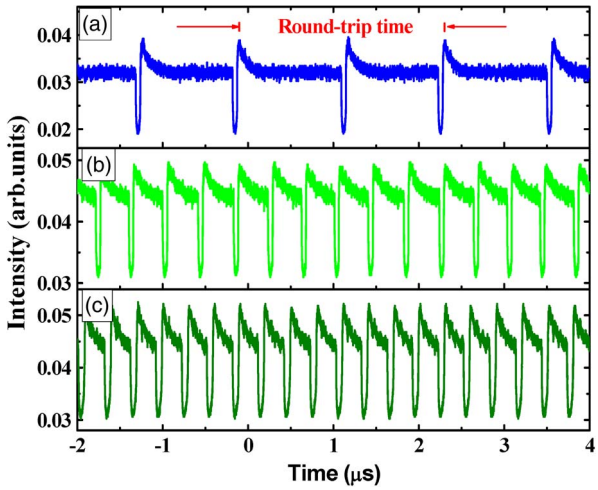

Fig. 7. Operation modes with the HML counterparts of dark square pulse of orders 2, 6, and 8 are shown in Fig. 5(a)–(c).

duration becomes narrower as the pump power increases. At a maximum pump power of 600 mW, the dark square pulse bunches and HML are also obtained by tuning the PC to different orientations. Furthermore, distinct operation regimes can be achieved in same GOSA when slightly changing the pump power and the polarization status in cavity.

References

[1] K. Tamura, E. P. Ippen, H. A. Haus, and L. E. Nelson, "77-fs pulse generation from a stretched-pulse mode-locked all-fiber ring laser," *Opt. Lett.*, vol. 18, no. 13, pp. 1080–1082, Jul. 1993.
[2] T. Tsai and Y. Fang, "A saturable absorber Q-switched all-fiber ring laser," *Opt. Exp.*, vol. 17, no. 3, pp. 1429–1434, Feb. 2009.
[3] V. E. Zakharov and A. B. Shabat, "Interaction between solitons in a stable medium," *Sov. Phys.—JETP*, vol. 37, no. 823, pp. 823–828, Dec. 1973.
[4] W. van Saarloos and P. C. Hohenberg, "Fronts, pulses, sources and sinks in generalized complex Ginzburg-Landau equations," *Phys. D, Nonlin. Phenom.*, vol. 56, no. 4, pp. 303–367, Jun. 1992.
[5] N. Bekki and K. Nozaki, "Formations of spatial patterns and holes in the generalized Ginzburg-Landau equation," *Phys. Lett. A*, vol. 110, no. 3, pp. 133–135, Jul. 1985.
[6] Y. S. Kivshar and G. P. Agrawal, *Optical Solitons: From Fibers to Photonic Crystals*. San Diego, CA, USA: Academic, 2003.
[7] G. Agrawal, *Applications of Nonlinear Fiber Optics*. Amsterdam, The Netherlands: Elsevier, 2001.
[8] Y. S. Kivshar and B. Luther-Davies, "Dark optical solitons: Physics and applications," *Phys. Rep.*, vol. 298, no. 2/3, pp. 81–197, May 1998.
[9] J. Wallace, *Laser From NIST/JILA Directly Produces Picosecond Dark Pulses [EB/OL]*, 2010. [Online]. Available: http://www.laserfocusworld.com/articles/2010/06/laser-from-nist-jila.html
[10] W. H. Oskay *et al.*, "Single-atom optical clock with high accuracy," *Phys. Rev. Lett.*, vol. 97, no. 2, pp. 020801-1–020801-4, Jul. 2006.
[11] M. Quiroga-Teixeiro, C. B. Clausen, M. P. Srensen, P. L. Christiansen, and P. A. Andrekson, "Passive mode locking by dissipative four-wave mixing," *J. Opt. Soc. Amer. B, Opt. Phys.*, vol. 15, no. 4, pp. 1315–1321, Apr. 1998.
[12] T. Sylvestre, S. Coen, P. Emplit, and M. Haelterman, "Self-induced modulational instability laser revisited: Normal dispersion and dark-pulse train generation," *Opt. Lett.*, vol. 27, no. 7, pp. 482–484, Apr. 2002.
[13] H. Zhang, D. Y. Tang, L. M. Zhao, and X. Wu, "Dark pulse emission of a fiber laser," *Phys. Rev. A*, vol. 80, no. 4, pp. 045803-1–045803-4, Oct. 2013.
[14] H. Zhang, D. Tang, M. Tlidi, L. Zhao, and X. Wu, "Dispersion-managed dark solitons in erbium-doped fiber lasers," *arXiv preprint arXiv:1007.3129*, 2010.
[15] H. S. Yin, W. C. Xu, A. P. Luo, Z. C. Luo, and J. R. Liu, "Observation of dark pulse in a dispersion-managed fiber ring laser," *Opt. Commun.*, vol. 283, no. 21, pp. 4338–4341, Nov. 2010.
[16] M. Haelterman and M. Badolo, "Dual-frequency wall solitary waves for nonreturn-to-zero signal transmission in W-type single-mode fibers," *Opt. Lett.*, vol. 20, no. 22, pp. 2285–2287, Nov. 1995.
[17] M. Haelterman and A. P. Sheppard, "Polarization domain walls in diffractive or dispersive Kerr media," *Opt. Lett.*, vol. 19, no. 2, pp. 96–98, Jan. 1994.
[18] H. Zhang, D. Y. Tang, L. M. Zhao, and R. J. Knize, "Vector dark domain wall solitons in a fiber ring laser," *Opt. Exp.*, vol. 18, no. 5, pp. 4428–4433, Mar. 2009.

[19] H. Zhang, D. Tang, L. Zhao, and X. Wu, "Dual-wavelength domain wall solitons in a fiber ring laser," *Opt. Exp.*, vol. 19, no. 4, pp. 3525–3530, Feb. 2010.
[20] D. Y. Tang *et al.,* "Evidence of dark solitons in all-normal-dispersion-fiber lasers," *Phys. Rev. A*, vol. 88, no. 1, pp. 013849-1–013849-6, Jul. 2013.
[21] W. Gao, M. Liao, H. Kawashima, T. Suzuki, and Y. Ohishi, "Dark-square-pulse generation in a ring cavity with a tellurite single-mode fiber," *IEEE Photon. Technol. Lett.*, vol. 25, no. 6, pp. 546–549, Mar. 2013.
[22] L. Wang *et al.,* "Dark pulses with tunable repetition rate emission from fiber ring laser," *Opt. Commun.*, vol. 285, no. 8, pp. 2113–2117, Apr. 2012.
[23] X. Li, S. M. Zhang, Y. C. Meng, and Y. P. Hao, "Harmonic mode locking counterparts of dark pulse and dark-bright pulse pairs," *Opt. Exp.*, vol. 21, no. 7, pp. 8409–8416, Apr. 2013.
[24] F. Bonaccorso, Z. Sun, T. Hasan, and A. C. Ferrari, "Graphene photonics and optoelectronics," *Nat. Photon.*, vol. 4, no. 9, pp. 611–622, Sep. 2010.
[25] K. P. Loh, Q. Bao, G. Eda, and M. Chhowalla, "Graphene oxide as a chemically tunable platform for optical applications," *Nat. Chem.*, vol. 2, no. 12, pp. 1015–1024, Dec. 2010.
[26] G. Sobon *et al.,* "Graphene oxide vs. reduced graphene oxide as saturable absorbers for Er-doped passively mode-locked fiber laser," *Opt. Exp.*, vol. 20, no. 17, pp. 19 463–19 473, Aug. 2012.
[27] J. Xu, J. Liu, S. D. Wu, Q. H. Yang, and P. Wang, "Graphene oxide mode-locked femtosecond erbium-doped fiber lasers," *Opt. Exp.*, vol. 20, no. 14, pp. 15 474–15 480, Jul. 2012.
[28] Z. B. Liu, X. Y. He, and D. N. Wang, "Passively mode-locked fiber laser based on a hollow-core photonic crystal fiber filled with few-layered graphene oxide solution," *Opt. Lett.*, vol. 36, no. 16, pp. 3024–3026, Aug. 2011.
[29] X. Zhao, Z. B. Liu, W. B. Yan, Y. P. Wu, X. L. Zhang, Y. S. Chen, and J. G. Tian, "Ultrafast carrier dynamics and saturable absorption of solution-processable few-layered graphene oxide," *Appl. Phys. Lett.*, vol. 98, no. 12, pp. 121905-1–121905-3, Mar. 2011.
[30] Y. G. Wang, H. R. Chen, X. M. Wen, W. F. Hsieh, and J. Tang, "A highly efficient graphene oxide absorber for Q-switched Nd: GdVO4 lasers," *Nanotechnology*, vol. 22, no. 45, p. 455203, Nov. 2011.
[31] J. Q. Zhao, Y. G. Wang, P. G. Yan, S. C. Ruan, J. Q. Cheng, G. G. Du, Y. Qin. Yu, G. L. Zhang , H. F. Wei, and J. Luo, "Graphene-oxide-based Q-switched fiber laser with stable five-wavelength operation," *Chin. Phys. Lett.*, vol. 29, no. 11, p. 114206, Nov. 2012.
[32] J. Q. Zhao, Y. G. Wang, P. G. Yan, S. C. Ruan, G. L. Zhang, H. Q. Li, and Y. H. Tsang, "An L-band graphene-oxide mode-locked fiber laser delivering bright and dark pulses," *Laser Phys.*, vol. 23, no. 7, p. 075105, Jul. 2013.
[33] E. Seve, G. Millot, S. Wabnitz, T. Sylvestre, and H. Maillotte, "Generation of vector dark-soliton trains by induced modulational instability in a highly birefringent fiber," *J. Opt. Soc. Amer. B, Opt. Phys.*, vol. 16, no. 10, pp. 1642–1650, Oct. 1999.
[34] J. Q Zhao, P. G. Yan, and S. C. Ruan, "Observations of three types of pulses in an erbium-doped fiber laser by incorporating a graphene saturable absorber," *Appl. Opt.*, vol. 52, no. 35, pp. 8465–8470, Dec. 2013.
[35] P. Grelu, F. Belhache, F. Gutty, and J. M. Soto-Crespo, "Relative phase locking of pulses in a passively mode-locked fiber laser," *J. Opt. Soc. Amer. B, Opt. Phys.*, vol. 20, no. 5, pp. 863–870, May 2003.